Role of defects in the metal-insulator transition in VO_{2} and V_{2}O_{3}

Darshana Wickramaratne, Noam Bernstein, and I. I. Mazin

Phys. Rev. B **99**, 214103 — Published 7 June 2019

DOI: 10.1103/PhysRevB.99.214103

The role of defects in the metal-insulator transition in VO_2 and V_2O_3

Darshana Wickramaratne,[1] Noam Bernstein,[2] and I. I. Mazin[2]

[1] *NRC Research Associate, Resident at Center for Computational Materials Science, US Naval Research Laboratory, Washington, D.C. 20375, USA*

[2] *Center for Computational Materials Science, US Naval Research Laboratory, Washington, DC 20375, USA*

(Dated: May 6, 2019)

The vanadates VO_2 and V_2O_3 are prototypical examples of strongly correlated materials that exhibit a metal-insulator transition. While the phase transitions in these materials have been studied extensively, there is a limited understanding of how the properties of these materials are affected by the presence of defects and doping. In this study we investigate the impact of native point defects in the form of Frenkel defects on the structural, magnetic and electronic properties of VO_2 and V_2O_3, using first-principles calculations. In VO_2 the vanadium Frenkel pairs lead to a non-trivial insulating state. The unpaired vanadium interstitial bonds to a single dimer, which leads to a trimer that has one singlet state and one localized single-electron $S = 1/2$ state. The unpaired broken dimer created by the vanadium vacancy also has a localized $S = 1/2$ state. Thus, the insulating state is created by the singlet dimers, the trimer and the two localized $S = 1/2$ states. Oxygen Frenkel pairs, on the other hand, lead to a metallic state in VO_2, but are expected to be present in much lower concentrations. In contrast, the Frenkel defects in V_2O_3 do not directly suppress the insulating character of the material. However, the disorder created by defects in V_2O_3 alters the local magnetic moments and in turn reduces the energy cost of a transition between the insulating and conducting phases of the material. We also find self-trapped small polarons in V_2O_3, which has implications for transport properties in the insulating phase.

I. INTRODUCTION

V_2O_3 and VO_2 are prototypical strongly correlated materials that exhibit a metal-insulator transition (MIT).[1,2] The MIT in V_2O_3 and VO_2 manifests itself as a change in resistivity of several orders of magnitude. Furthermore, the phase transition in these materials is accompanied by a concomitant structural (and magnetic in the case of V_2O_3) transition. At a temperature of 155 K V_2O_3 transitions from a high-temperature (HT) paramagnetic metallic corundum phase to a low-temperature (LT) antiferromagnetic insulating monoclinic phase. VO_2, in contrast, is non-magnetic, and exhibits a transition from a HT metallic rutile structure to a LT insulating monoclinic structure at 340 K.[3] The interplay between the electronic, structural and magnetic degrees of freedom in these materials has led to a number of studies that have sought to exploit the sensitivity of these phase transitions to the application of strain,[4] pressure,[5] doping[6,7] and the introduction of defects.[8,9]

Despite several decades of research, the ability to manipulate the transition temperature in these materials remains a challenge due to the lack of a quantitative description of how the MIT responds to external stimuli. This is reflected in the results of recent experiments,[9] where the response of the MIT to ion irradiation was shown to be qualitatively different in V_2O_3 as compared with VO_2. V_2O_3 and VO_2 thin films were subjected to ion irradiation at different dosage levels. The electronic properties of the two materials showed markedly different properties pre and post irradiation. Prior to irradiation, both vanadate thin films exhibited a MIT as evidenced by a large change in electrical resistivity across the respective transition temperature of the two materials. Post-irradiation, the transition temperature was observed to decrease in V_2O_3 while the magnitude of the resistivity on both sides of the transition temperature remained unchanged compared to the unirradiated sample. At a critical irradiation dosage, the MIT in V_2O_3 was completely suppressed and the electrical resistivity exhibited metallic-like conduction. In contrast, the MIT phenomenon in VO_2 appeared to be more robust. The transition temperature post-irradiation remained unchanged compared to the unirradiated sample while the resistivity below the transition temperature decreased by approximately two orders of magnitude. At higher dosages of irradiation, evidence of a MIT in VO_2 remained, although the magnitude of the resistivity change between the insulating and conducting state was lower compared to the unirradiated sample. In both vanadates, there was no evidence of structural distortion or strain introduced as a result of the irradiation. Hence, it is likely that any changes observed in the MIT phenomenon in the two materials is due to the introduction of defects. A crucial question then is, what is the microscopic origin of the different response of the MIT in both materials to the presence of defects?

Point defects can affect the electronic structure through a multitude of mechanisms. One possibility is that the defects act as sources of free carriers which would lead to appreciable conductivity below the MIT temperature and a collapse in the MIT. Another possibility is that the presence of defects introduces structural disorder. A *quantitative* description of the impact of these effects on the MIT in the vanadates will need to accurately account for the role of strong correlations and the structural, electronic and magnetic properties of each material.

The above overview makes it clear that aspects related

to the role of defects in the vanadates remain to be explored. Motivated by this, we use first-principles density functional theory (DFT) calculations to determine the electronic, magnetic and structural properties of defects in V_2O_3 and VO_2.

A. General considerations

The chemical simplicity of V_2O_3 and VO_2 led to a majority of the initial research effort devoted to these materials to assume an oversimplified view of their electronic structure, where V_2O_3 was treated as a prototypical Mott insulator and VO_2 as a Peierls insulator. However, intensive and decades-long research has shattered this deceptive simplicity and an understanding has gradually emerged that (i) the MIT in the two vanadates have very different properties and (ii) in each case, several different physical phenomena contribute. In the following we will present this understanding and how it has emerged on a qualitative level (as a result of numerous quantitative calculations with complementary methodologies).

In VO_2, the vanadium ion is in a 4^+ oxidation state, that is, it has 1 d-electron. The HT crystal structure of VO_2 has a high symmetry rutile structure, which does not allow for an insulator, except for a Mott insulator. Oxygen forms nearly perfect octahedra around the V ions, thus splitting the V d states into a well separated t_{2g} triplet and e_g doublet (cf. Fig. 1(a)). First-principles calculations show that a Hubbard parameter $U - J \gtrsim 2$ eV opens an antiferromagnetic Mott-Hubbard gap at $T = 0$.[10] However, this phase exists only above 340 K, which is above its intrinsic Néel temperature, so experimentally it is always paramagnetic and metallic. Deviation from antiferromagnetic order strongly suppresses the tendency toward insulating behavior; indeed, in a ferromagnetic arrangement the Hubbard gap only opens at a larger value $U - J \gtrsim 3.5$ eV. It is worth noting that the electronic structure of VO_2 in the metallic phase does not exhibit any nesting features that would trigger a conventional, Fermi-surface driven charge density wave and dimerization of the structure. Indeed, the LT structure is not really reminiscent of a charge density wave, but rather exhibits strongly coupled dimers with the V-V distance along the c-axis changing from uniform separation of 2.85 Å to alternating dimers with bond lengths of 2.65 Å and 3.12 Å, which is also accompanied by a strong trigonal distortion of approximately 30%.[11] This trigonal distortion splits the nearly-degenerate t_{2g} orbitals[12] into an elongated a_{1g} singlet and a more isotropic e_g' doublet (cf. Fig. 1(a)). The a_{1g} orbitals in each dimer point toward each other and form a strong covalent bond.[13] In an ionic picture, this bond is occupied by two electrons forming a typical covalent singlet (analogous to a H_2 molecule) and a gap opens between this covalent state and the lowest e_g' state (cf. Fig. 1(a))

In a solid, these states broaden into bands. Describing these bands with the use of local and semilocal functionals such as the local density approximation (LDA) or the generalized gradient approximation (GGA) within DFT leads to bandwidths that are overestimated and their relative separation is underestimated, a manifestation of the well known "band gap" problem in DFT.[14,15] While there are many remedies to this effect, such as DFT+U, dynamical mean field theory (DMFT), hybrid functionals, or meta-GGA functionals such as the MBJ functional or the recently developed SCAN functional, which indeed all open a gap in VO_2,[10,16,17] all of them simultaneously increase the propensity toward magnetism and disrupt the formation of singlet dimers (DFT-like theory can only describe a single-determinant state, and not a true singlet). *Cluster* dynamical mean field theory (DMFT), on the contrary, has this capability, but is too computationally expensive to be applied to large supercells.[12,18] Fortunately, non-magnetic GGA calculations, as discussed in more detail below, yield a structure rather close to the experimentally observed structure, only slightly overestimating the degree of dimerization. This behavior can be used, in some cases, to circumvent the problem by optimizing the atomic structure using one method and interrogating the electronic structure using another.

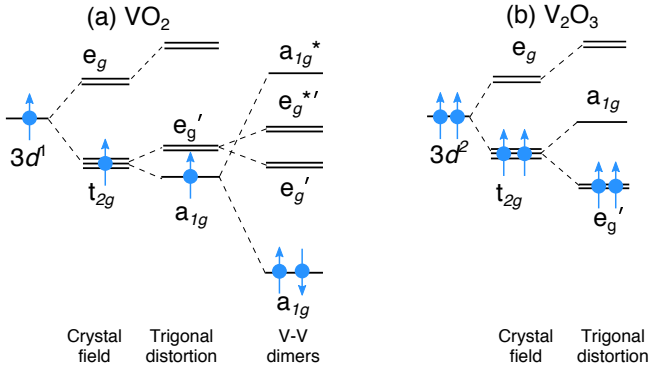

FIG. 1. Schematic of the energy levels of vanadium d-states and their occupation in (a) VO_2 and (b) V_2O_3. For VO_2 the single $3d^1$ state subject to an octahedral crystal field, trigonal distortion and the energy separation between the bonding a_{1g} and antibonding e_g^π orbitals due to covalent bonds between V dimers is illustrated. For V_2O_3 the ordering of the two $3d^2$ states subject to an octahedral crystal field and trigonal distortion is illustrated.

The case of V_2O_3 is more subtle. The difference is that V is in the 3^+ oxidation state, which has two d-electrons that would not fit into one covalent bond. Thus, the dimerization mechanism described above is not operative (note that Ti_2O_3, having one electron less per Ti atom, *does* dimerize at low temperatures[19]). Prior studies have demonstrated[2,20] that the relatively small trigonal distortion in this compound also splits a_{1g} and e_g' states (cf. Fig. 1(b)), but this separation is considerably smaller than the bandwidths, at least on a one-electron level. Hence, in DFT calculations it is a metal. Importantly, the doubly degenerate e_g' orbitals are lower in energy than the a_{1g} ones, so any interaction that amplifies the $e_g' - a_{1g}$

splitting opens a gap in V_2O_3 with its 2 d-electrons per V. Since all of the relevant orbitals are localized on a single V site, the DFT+U method is well suited for describing this effect. Note that the physics that leads to the insulating state here is very different from that in VO_2. Furthermore, it was recently shown that the MIT in V_2O_3 in itself is not a Mott transition at all, even though it is a transition between a Mott insulator and a correlated metal.[21,22] Rather, it is a strongly-first order transition between two systems that are different in more aspects than just their electronic structure. Specifically, the magnetic interactions in the HT corundum phase are strongly frustrated, and if the structural transition upon cooling could have been arrested, the materials would have remained paramagnetic (and likely metallic) down to very low temperatures. Conversely, if the LT monoclinic structure could be stabilized well above 155 K, it would have remained an ordered Mott antiferromagnet well above room temperature. This suggests that the MIT in V_2O_3 should be more sensitive to structural aspects than in VO_2.

Some first-principles studies on strongly correlated oxides have highlighted the important effect structural disorder/defects may have on the energy barriers between different magnetic states.[23,24] Similarly, a recent study demonstrated that structural distortions associated with replacing V with Cr are responsible for enhanced correlation effects and stabilizing an insulating state at high temperatures.[25] It was also shown that despite Cr and V having different number of electrons such a replacement does not result in charge doping. Conversely, doping with Ti does result in charge doping, albeit, counterintuitively, in electron rather than hole doping. The response of V_2O_3 to this charge doping is that expected for a true Mott insulator, that is, it rapidly transforms into a correlated metal.

B. Outline

In this study we investigate the points defects that are likely to be introduced by ion irradiation[9] by considering the properties of a neutral Frenkel defect, i.e. a self-interstitial and a corresponding (but not adjacent) vacancy that form due to an atomic displacement, in V_2O_3 and VO_2. We also examine the role of pure electron and hole doping by introducing electrons and holes with overall charge neutrality ensured by a uniform compensating background. Investigating these effects separately allows us to capture the physics of charge doping in isolation from the effects of atomic disorder as introduced by the presence of defects.

The relatively complete understanding of the physics of pristine and doped V_2O_3 and VO_2 suggests a straightforward qualitative explanation of the qualitatively different responses of the two compounds when subject to irradiation. Irradiation displaces a small fraction of ions. If we consider the displacement of V ions, this will result in the creation of vanadium Frenkel pairs, where the diplaced V ions and the newly formed vacancies are not on nearest-neighbor sites.

In the case of VO_2, breaking a V dimer results in two unpaired V ions, while, presumably, leaving the other dimers relatively intact (in the following sections we will quantify this statement) and they will remain covalent singlets. The unpaired V ions, assuming that they do not change their valence (again, we will quantify this statement later), will have one d-electron each, subject to Hubbard correlations, and will form isolated $S = 1/2$ impurities, localized by the Hubbard interaction. The material will thus remain insulating (but, if it will be possible to measure the magnetic response sufficiently accurately, we expect the material to exhibit a Curie-like spin susceptibilty with an effective moment of $2\sqrt{S(S+1)} = \sqrt{3}$ μ_B per unpaired V atom). Our calculations confirm these general considerations with one additional interesting observation: the unpaired vanadium interstitial bonds to one of the dimers forming a covalently bonded trimer. This trimer has one localized $S = 1/2$ unpaired state that is subject to Hubbard correlations. Furthermore, applying a reasonable U to VO_2 with the vanadium Frenkel pair leads to a band gap that is significantly suppressed compared to the band gap of pristine VO_2. This is consistent with the experimental observation that upon irradiation of VO_2, the MIT is preserved but the resistivity in the insulating phase decreases by up to two orders of magnitude compared to pristine VO_2. In contrast, we find that oxygen Frenkel pairs lead to a metallic state. However, the formation energy of the oxygen Frenkel pairs is high. Hence, we expect them to exist at lower concentrations and in turn not affect the macroscopic transport properties of VO_2 significantly. For the case of VO_2 we only focus on the properties of Frenkel defects in the insulating monoclinic phase since our goal is to address how robust the insulating state and the vanadium dimerization is to the presence of native defects.

Our considerations of the electronic structure of V_2O_3 would suggest the crystal field, and therefore the valence state, of V in V_2O_3 is rather sensitive to local structural distortions. If (and we will see that this is indeed the case) displaced V ions in V_2O_3 acquire a different valence state, one may expect this to result in charge doping and presumably a rapid suppression of the MIT temperature, analogous to Ti-doped V_2O_3.[25] Our calculations, presented below, partially confirm this picture, but also uncover unexpected insight. Most importantly, the calculations suggest that for a low concentration of Frenkel pairs (as low as in experiment[9]), the extra charge does not become itinerant. Instead, the extra charge localizes on a single vanadium atom, alters the V-O bond length and leads to the formation of a localized small polaron. Furthermore, while the presence of Frenkel defects does not lead to a doping driven suppression of the Mott insulating state in V_2O_3, we find the Frenkel pairs reduce the energy cost of the transition between the LT and HT magnetic states. This reduction in the energy to

transition between the magnetic states is consistent with the experimental observation that in V_2O_3 the MIT temperature decreases upon irradiation.

In Sec. II we describe the computational methodology. In Sec. III A we discuss the structural and electronic properties of VO_2 and V_2O_3. The properties of defects in VO_2 are described in Sec. III B and the properties of defects in V_2O_3 are described in Sec. III C. Key results from our study are summarized in Sec. IV.

II. COMPUTATIONAL METHODS

Our calculations are based on density functional theory within the projector-augmented wave method[26] as implemented in the VASP code[27,28] using the generalized gradient approximation defined by the Perdew-Burke-Ernzerhof (PBE) functional.[29] In our calculations, V $4s^2 3p^6 3d^3$ electrons and O $2s^2 2p^4$ electrons are treated as valence. All calculations use a plane-wave energy cutoff of 600 eV. For the calculations in the primitive unit cells we use an $8\times8\times8$ k-point grid. In order to simulate the Mott-insulating behavior of V_2O_3 and to capture the role of strong correlations in VO_2 we use a spherically-averaged Hubbard correction within the fully-localized limit double-counting subtraction.[30] All of the DFT+U calculations for VO_2 and V_2O_3 relied on the PBE functional. In the case of VO_2, we optimize the volume and atomic coordinates of the unit cell and the defect supercell using non-spin polarized PBE calculations. Subsequent calculations of the VO_2 electronic structure that use the PBE optimized structure are based on DFT+U. For the case of V_2O_3, all of our calculations are based on DFT+U. We apply a $U-J$ value of 1.8 eV to the V d-states for the calculations of V_2O_3 and a $U-J$ value of 2 eV to the V d-states in the case of VO_2. These parameters yield the closest agreement with the experimental band gaps in both materials.

Calculations of defects in both materials relied on the supercell approach. For the lowest-energy defect geometries we use quasi-cubic supercells with 324 atoms for VO_2 and 360 atoms for V_2O_3. The 324 atom VO_2 supercells are comprised of 108 VO_2 formula units, which in turn leads to a Frenkel pair concentration of 0.92% in our calculations. The 360 atom V_2O_3 supercells are comparised of 144 V_2O_3 formula units which leads to a Frenkel pair concentration of 0.69% in our calculations. In order to scan several less favorable geometries we used smaller supercells of 96 atoms for VO_2 and 160 atoms for V_2O_3. Calculations with these small VO_2 and V_2O_3 defect supercells were performed on $2\times2\times2$ k-point grids while for the largest supercells only the Γ-point was used to optimize the structure and obtain total energies and densities of states.

We identify the most favorable defect configuration by evaluating several configurations of Frenkel pairs in each vanadate. To generate the initial geometry for these configurations we find maximally large spherical voids in the primitive cell. For each spherical void we place an interstitial in the center, and pick the farthest site of the same species (considering the effects of the periodic boundaries) for the vacancy. We then relax the configuration with respect to atomic positions and unit cell size and shape. The resulting formation energy of, for example, an oxygen Frenkel pair in V_2O_3, is defined as:

$$E^f(\mathrm{O}_i{-}v_\mathrm{O}) = E_\mathrm{tot}(O_i{-}v_\mathrm{O}) - E_\mathrm{tot}(\mathrm{V_2O_3}) \qquad (1)$$

where $E_\mathrm{tot}(\mathrm{O}_i\text{-}v_\mathrm{O})$ denotes the total energy of the V_2O_3 defect supercell with an oxygen interstitial, O_i and an oxgen vacancy, v_O. $E_\mathrm{tot}(V_2O_3)$ is the total energy of the pristine V_2O_3 supercell. Since we only consider Frenkel pairs in this study, the formation energy is not dependent on the atomic chemical potential. We also consider the formation energy of charged Frenkel pairs in the singly negative and positive charge states and find them to be higher in energy than the neutral Frenkel pair. Unless otherwise stated, we only report on the results of geometries for neutral Frenkel pairs in each material that have the lowest formation energy.

We also investigate the formation of self-trapped small polarons in pristine V_2O_3. In the case of small hole polarons we remove an electron from the pristine supercell of each material, perturb the initial magnetic moment on a single V atom, decrease the V-O bond length around the single V atom with respect to the equilibrium V-O bond length and then allow for a complete relaxation of all atomic coordinates. In the case of small electron polarons we add an electron to the defect supercell, perturb the magnetic moment around a single V atom and increase the V-O bond length around the V site before allowing for a complete relaxation of all atomic coordinates. Note that investigation of self-trapped polarons in VO_2 is not possible with the DFT+U calculations used in this study, for the technical reasons outlined in Sec. I A. Namely, small polarons must be magnetic and require full account of Hubbard correlations, but any account of correlations at the level below cluster DMFT overestimates the tendency to magnetism and kills the dimerization.

III. RESULTS

A. Defect-free structures

We first report on the electronic structure of VO_2. For the LT monoclinic phase of VO_2, we find that a non-spin-polarized PBE-functional relaxation leads to good agreement with experiment for both the unit cell lattice constants and V dimerization distance. The relaxed lattice constants are $a = 5.631$ Å, $b = 4.541$ Å and $c = 5.254$ Å, which are within 2.3% of the experimentally reported lattice constants for monoclinic VO_2: $a = 5.750$ Å, $b = 4.540$ Å and $c = 5.380$ Å.[11] The V atoms form dimers where the V short bond length is 2.515 Å, consistent with x-ray diffraction measurements of 2.62 Å.[11]

In contrast, relaxing the atomic coordinates and the volume of the VO_2 monoclinic unit cell using DFT+U enhances the tendency for the V atoms to become magnetic and leads to equally spaced V atoms along the c-axis. However, the electronic structure from a DFT+U calculation of a monoclinic VO_2 structure optimized using a non-spin polarized PBE calculation yields good agreement with experiment. The $U - J$ value of 2 eV we use in our calculations leads to a band gap of 0.68 eV, which is in close agreement with the experimental band gap of 0.60 eV determined by infra-red absorption[31] measurements. The density of states (DOS) of VO_2 in its insulating monoclinic phase is plotted in Fig. 2(a). The valence band is comprised of hybridized V d-states and O p-states while the bottom of the conduction band primarily consists of V d-states.

For V_2O_3 we investigate the high-temperature (HT) and low-temperature (LT) phases. To describe the antiferromagnetic configuration of the LT monoclinic phase of V_2O_3 we use a four formula-unit cell. We find the ground state magnetic order to be one where the magnetic moments are ferromagnetically aligned within the a-c plane of the monoclinic structure and are antiferromagnetically aligned along the monoclinic b axis, consistent with neutron scattering studies of V_2O_3 and previous calculations in the insulating phase.[22,32] The atomic coordinates, shape and volume of the unit cell are optimized using DFT+U with the parameters outlined in Sec. II. We find the lattice constants of the LT monoclinic structure of V_2O_3 to be a = 7.414 Å, b = 5.084 Å and c = 5.559 Å, which is within 2.1% of the experimental LT lattice constants (a = 7.255 Å, b = 5.002 Å and c = 5.548 Å) reported for monoclinic V_2O_3.[33] The density of states for the LT monoclinic phase of V_2O_3 is plotted in Fig. 2(b). The top of the valence band in V_2O_3 is comprised of V d-states with a minor contribution from O p-states. The bottom of the conduction band is composed entirely of V d-states. Our DFT+U calculations of monoclinic V_2O_3 yield a band gap of 0.35 eV, which is close to the band gap of ∼0.40 eV obtained from optical conductivity measurements in V_2O_3.[31]

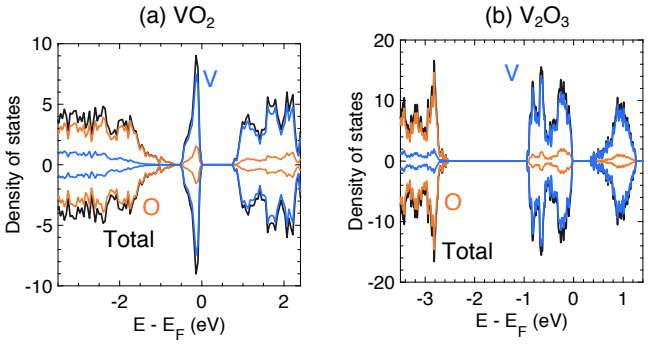

FIG. 2. Density of states for the monoclinic insulating phase of (a) VO_2 and (b) V_2O_3. The majority spin states are illustrated with positive values and the minority spin states are illustrated with negative values

We use a two formula-unit cell for the HT metallic corundum phase of V_2O_3. Neutron scattering studies have shown this phase to be a highly frustrated paramagnet.[22] Description of such a state is always a challenge in DFT, because the existence of the fluctuating local moments is essential for structural properties (cf. Fe-based superconductors), but the standard DFT can only describe either non-magnetic (not *para*magnetic!) or magnetically ordered states. Fortunately, as shown in Ref. 22, the corundum phase of V_2O_3 is magnetically frustrated so magnetic ordering must affect the total energy only weakly. Of the possible ordered phases we have selected the ferromagnetic one as a proxy for a magnetically disordered state because it respects the same full lattice symmetry (as opposed to antiferromagnetic arrangements). We use the same $U - J$ value of 1.8 eV as before. Optimizing the atomic coordinates, shape and volume of the ferromagnetic corundum unit cell using DFT+U leads to the following lattice constants: a = 5.0375 Å and c = 14.305 Å. This is within 2.1% of the experimental lattice constants, a = 4.952 Å and c = 14.003 Å, of the corundum phase of V_2O_3 measured using x-ray diffraction at room temperature.[33] The structural parameters for VO_2 and V_2O_3 are summarized in Table I.

To determine the most favorable magnetic configuration of either pristine V_2O_3 or V_2O_3 with defects we calculate a spin-flip energy $\Delta E = E_{tot}(AFM) - E_{tot}(FM)$, where $E_{tot}(AFM)$ and $E_{tot}(FM)$ are the total energies of the V_2O_3 **unit cell or** supercell with the V atoms antiferromagnetically and ferromagnetically aligned, respectively. Hence, negative spin-flip energies correspond to the antiferromagnetic configuration being favored. The spin-flip energy between antiferromagnetic and ferromagnetic phase of corundum V_2O_3 (allowing for full relaxation of the atomic coordinates, cell shape and volume) is only 0.0037 eV per V_2O_3 **unit cell** (or 10 K per V). This is consistent with the notion that the system is magnetically frustrated and its ordering temperature would be well below the temperature range where it exists in na-

TABLE I. Lattice constants, monoclinic and rhombohedral bond angles and space group for VO_2 and V_2O_3, comparing the calculated DFT+U results with experimentally reported data.

Material	Method	a (Å)	b (Å)	c (Å)	Bond angle (θ)	Space group
Monoclinic VO_2	DFT+U	5.631	4.541	5.254	121.9	$P2_1/c$
	Expt.[11]	5.752	4.537	5.382	122.6	
Monoclinic V_2O_3	DFT+U	7.414	5.084	5.559	97.3	C_2/c
	Expt.[33]	7.255	5.002	5.548	96.8	
Corundum V_2O_3	DFT+U	5.037		14.305	54.6	R-3c
	Expt.[33]	4.952		14.003	56.1	

ture, just as found by Leiner *et al.*[22]

We note that there is a principal physical difference between the MIT in the two vanadates. In V_2O_3 it is controlled by the delicate energy balance between the two structurally *and magnetically* different phases. Hence, we focus on the impact defects have on their energies. In VO_2, the transition occurs at a higher temperature and does not involve magnetic order. A suppression of insulating behavior there, if any, can only occur through metallization of the LT monoclinic phase, so in this study we only concentrated on studying this phase in VO_2 in the presence of defects.

B. VO_2 defects

We consider the properties of V and O Frenkel pairs in VO_2, optimizing the defect supercell using non-spin polarized PBE calculations. We start with the V Frenkel pair, where we find that the unpaired vanadium interstitial bonds to one of the V-V dimers forming a nearly equilateral triangle with a V-V bond length of ∼2.50 Å. Furthermore, as illustrated in Fig. 3(a), the unpaired V interstitial is also octahedrally coordinated by the nearest neighbor oxygen atoms; the V-O bond lengths range from 1.89 Å to 2.05 Å, which are close to the V-O bond lengths of pristine VO_2. We investigated several positions of the unpaired vanadium self interstitial and find this configuration, where it bonds to a single dimer, to be the most stable, with a formation energy of 3.67 eV. The V vacancy breaks a dimer leaving behind an unpaired V atom, and leads to oxygen dangling bonds that disrupt the V dimerization near the vacancy site. We therefore report results for large supercells with more than 100 VO_2 formula units, which maintain the dimerization of the vanadium atoms far from the vacancy site, unless otherwise noted.

The geometry of the unpaired vanadium interstitial can be understood from the following analysis, starting from a dimer and an isolated ion. As discussed above, the dimer forms a doubly occupied bonding state at $-t_{dd\sigma}$, where $t_{dd\sigma}$ is the hopping (direct overlap) between a_{1g} orbitals, and several nonbonding and antibonding states. Since the electron of the isolated atom is in a nonbonding state, at this level of approximation the noninteracting electron energy of the three ions in question is $-2t_{dd\sigma}$. Arranging the ions in a triangle creates one bonding state at $-2t_{dd\sigma}$, in addition to some non-bonding and antibonding states. Populating the bonding state with two electrons and a non-bonding state with the third electron leads to an electron energy gain of $-4t_{dd\sigma}$. This configuration is clearly lower in energy than the original "dimer+isolated" arrangement. Indeed, our DOS calculations show two states with opposite spins, localized on this triangle, well below the Fermi level. The third electron may either stay on the triangle, in which case it becomes subject to Hubbard repulsion just as well as the electron localized on the isolated V ion, and does not contribute to conductivity. It can also move into the e'_g conductivity band and become metallic. Which case is realized is impossible to say on the model level, however, our DFT+U calculations, described below, indicate that a relatively small U readily creates an insulator. Indeed, our spin-polarized DFT+U calculations of the electronic structure of the V Frenkel lead to a band gap of 0.098 eV as seen in Fig. 3(b), albeit suppressed significantly in comparison to the band gap of pristine VO_2 (cf. Fig. 2(a)).

Thus, we conclude that upon irradiation the following, rather non-trivial insulating state is created. In addition to the singlet dimers away from the defects, it consists of one state with $S = 1/2$ localized on the unpaired broken-dimer neighbor of the vacancy, a singlet localized on the V triangle that includes the interstitial atom, and another $S = 1/2$ state localized on the same triangle. The reduction in the band gap due to the vanadium Frenkel pairs in VO_2 would lead to a lower electrical resistivity in the insulating phase compared to pristine VO_2. We note that this is consistent with electrical transport measurements on irradiated VO_2,[9] where the resistivity of VO_2 in the insulating phase decreased by up to two orders of magnitude upon irradiation compared to pristine VO_2.

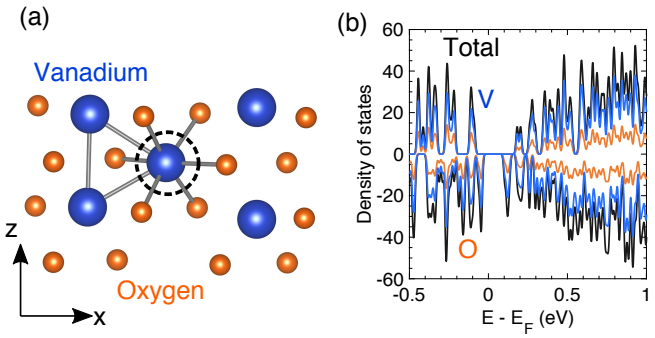

FIG. 3. (a) Schematic of the VO_2 supercell illustrating the vanadium self-interstitial (black dotted circle) that bonds with one of the V-V dimers. (b) Projected density of states for the LT monoclinic structure of VO_2 with a V Frenkel pair.

We also consider the role of oxygen Frenkel pairs in VO_2, where we find that the unpaired oxygen interstitial forms a bond with one vanadium atom. This oxygen is located 1.42 Å from one of the other oxygens coordinated to the same vanadium, forming a dimer (cf. Fig 4(a)), with oxygen-vanadium distances of 1.95 Å and 2.01 Å. The five remaining oxygens form V-O bonds with bond lengths that range from 1.84 Å to 2.01 Å. This configuration of the oxygen Frenkel leads to a formation energy of 4.86 eV, lowest among the various oxygen Frenkel configurations that we considered, but higher than that of the above-described V Frenkel of 3.67 eV.

O defects disrupt the crystal field of the nearest V ions, which in our calculations leads to closing of the gap, Fig. 4(b). However, the O Frenkel pairs have a higher formation energy and will have a much lower concentration compared to the V Frenkel pairs. Furthermore,

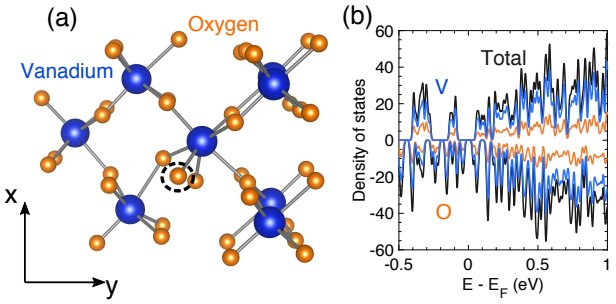

FIG. 4. (a) Schematic of the VO_2 supercell illustrating the oxygen self-interstitial (black dotted circle) that is a part of the oxygen Frenkel pair defect. (b) Projected density of states for the LT monoclinic structure of VO_2 with a O Frenkel pair

prior studies of ionic transport in semiconducting transition metal oxides have found the migration barrier for oxygen vacancies to be lower than the migration barrier of cation vacancies or cation self interstititials.[34,35] Hence, we also expect any O Frenkel pairs that may form in VO_2 to heal faster compared to the V Frenkel pairs. As a result we speculate O Frenkel defects will not affect the macroscopic transport properties of VO_2.

Thus far we have only considered the properties of the Frenkel defects with the lowest formation energy for either type of defects. It is conceivable that for the highest irradiation dosages Frenkel defects with higher formation energies can also be introduced.[9] Such high energy defects may have electronic properties that are different from the lowest energy Frenkel defect configurations that we have considered thus far. To this end, we also examined the electronic structure of the Frenkel defect configurations that have higher formation energies than the lowest energy configuration we have considered thus far (using, as described in Sec. II, smaller 96 atom supercells). In the case of the V Frenkel defects, we considered five other configurations of the V vacancy and self-interstitial pair that have formation energies up to 1.1 eV higher than the lowest energy configuration. We find the same qualitative features in the electronic and structural properties. The band gap is reduced with respect to the pristine material due to each defect. Due to the small sized supercell, we find the dimerization of the V atoms is no longer present. We also examined the electronic structure of five different configurations of O Frenkel defects that have formation energies up to 1 eV higher than the lowest energy defect. For each of these configurations, we also find the effects qualitatively similar to those with the lowest formation energies.

C. V_2O_3 defects

For V_2O_3 in the antiferromagnetic (and monoclinic low-T structure) or ferromagnetic (and corundum high-T structure) configuration the V interstitial relaxes to a position between two collinear c-axis aligned dimers. Figure 5(a) schematically illustrates the position of the V interstitial for the V Frenkel. The V atoms in this pentamer are all ferromagnetically aligned. The formation energy of the V Frenkel in the antiferromagnetic V_2O_3 supercell is 3.77 eV. We considered the possibility of the V Frenkel where the spin of the V interstitial is anti-aligned with the nearest neighbor V atoms and found it to have a higher formation energy of 3.98 eV. For the V Frenkel in the antiferromagnetic V_2O_3 supercell, we find a band gap of 0.27 eV (cf. Fig. 5(b)), which is lower than the band gap of pristine V_2O_3.

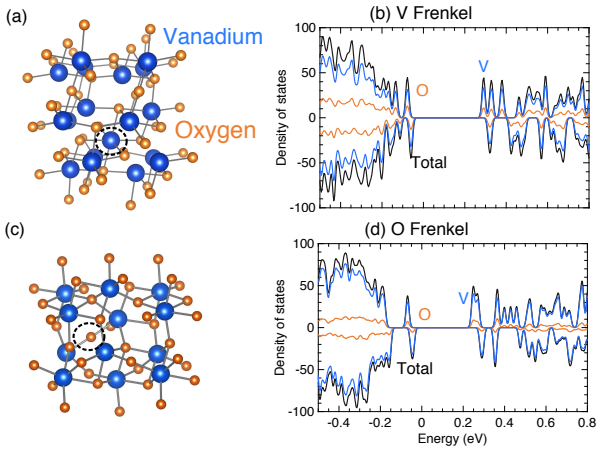

FIG. 5. (a) Schematic of the V_2O_3 supercell illustrating the vanadium self-interstitial (black dotted circle) that is a part of the vanadium Frenkel pair defect. (b) Projected density of states for the LT antiferromagnetic structure of V_2O_3 with the V Frenkel relative to the Fermi energy. (c) Schematic of the V_2O_3 supercell illustrating the oxygen self-interstitial (black dotted circle) that is a part of the oxygen Frenkel pair defect. (d) Projected density of states for the LT antiferromagnetic structure of V_2O_3 with the O Frenkel relative to the Fermi energy.

We also consider an oxygen Frenkel pair in V_2O_3. The oxygen interstitial that is a part of the O Frenkel pair leads to occupied states that are below the valence band and unoccupied states that are above the conduction band. The formation energy of the O Frenkel defect is 6.44 eV, which is higher than the formation energy of the V Frenkel pair. For the O Frenkel pair in the antiferromagnetic V_2O_3 supercell, we find V_2O_3 remains insulating with a band gap of 0.21 eV (cf. Fig. 5(d))

In addition to a possible direct effect on the band gap, defects in V_2O_3 may change the magnetic ordering energies and therefore affect the MIT, since it is coupled to the structural and magnetic transitions. For both Frenkel defects, we optimize the atomic coordinates of the **monoclinic** V_2O_3 supercell in a configuration where the undisplaced V atoms of the V_2O_3 supercell are ferromagnetically and antiferromagnetically aligned (taking into account the relaxed volumes of the two respective magnetic configurations). The former takes on the high-T corundum structure, while the latter takes on the low-T monoclinic structure. For pristine **monoclinic** V_2O_3,

TABLE II. Spin-flip energy, ΔE per V atom, between V_2O_3 in an antiferromagnetic configuration and in a ferromagnetic configuration obtained with 360 atom supercells.

Structure	ΔE per V atom (eV)
Pristine	-0.0065
V Frenkel	-0.0021
O Frenkel	-0.0038

the spin-flip energy, ΔE, is -0.0065 eV per V atom.

The spin-flip energy is -0.0021 eV per V atom in the supercell with a V Frenkel, and -0.0038 eV per V atom with an O Frenkel. Thus, the presence of either type of Frenkel pair defect in V_2O_3 lowers the spin flip energy relative to the pristine material. The results are summarized in Table II.

It is evident from Fig. 5(b) and Fig. 5(d) that the vanadium and oxygen Frenkel pairs do not suppress the V_2O_3 gap. However, both defects decrease the spin-flip energy and lower the energy cost of a transition to a metallic ferromagnetic state. This reduction in the spin-flip energy arises from the broken connectivity between the V atoms that are aligned antiferromagnetically along the *b*-axis. The local distortion introduced by the vacancy is sufficient to modify the magnetic moments of the dangling bond atoms. Furthermore, the self-interstitial in both Frenkel defects disrupts the magnetic moment of the nearest neighbor atoms that it bonds to. This combination of effects is sufficient to lower the spin-flip energy due to both types of Frenkel pairs that we consider here. As we discuss in Sec. I A and demonstrate with calculations of the spin-flip energy in Sec. III A, the HT phase of V_2O_3 is a highly frustrated paramagnet[22] with a low Néel temperature while the LT phase is strongly antiferromagnetic with a high Néel temperature. Hence, we suggest that this suppression in the energy cost due to the presence of defects arises primarily from an energy gain in the LT insulating phase of V_2O_3 that contains the Frenkel defects which shifts the energy balance towards the HT phase and is a plausible source for the reduction of the MIT temperature upon irradiation of V_2O_3.[9]

1. V_2O_3 polarons

The disruptions of the bonding caused by the V and O Frenkel pair defects in V_2O_3 also leads to hole doping due to changes in the valence state of the defect or near-defect atoms. However, these holes do not occupy band states, but instead localize through the formation of hole polarons. In the case of the V Frenkel pair, we find the formation of two hole polaron sites centered on two different V atoms. The effective oxidation state on these V atoms changes from V^{3+} to V^{4+}. The nearest neighbor V-O bond lengths of the hole polaron sites are 3% shorter than the equilibrium V-O bond length. This raises the question whether small hole and electron polarons can exist as isolated species in V_2O_3.

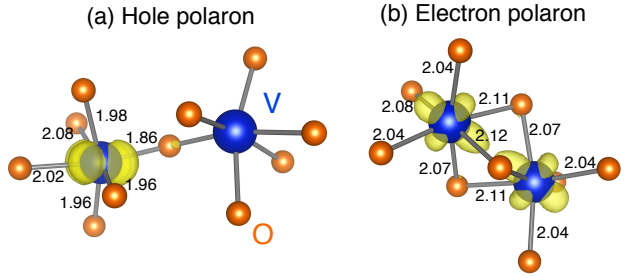

FIG. 6. Atomic configuration and the charge density isosurface for a small (a) hole polaron and (b) electron polaron in a V_2O_3 supercell. The V-O bond lengths around the polaron site are shown alongside each bond in units of Ångstroms.

To investigate small polarons in V_2O_3 we apply the approach described in Sec. II. We find small hole polarons to be stable in V_2O_3. The hole polaron localizes on a single V atom (along with a minor contribution from a nearest neighbor O atom), as illustrated in Fig. 6(a). The valence of the V atom changes from V^{3+} to V^{4+}. The formation of a small hole polaron leads to a distortion of the local geometry: we find the nearest neighbor V-O bonds that surround the polaron are 3 to 5% shorter than the equilibrium V-O bond length. The self-trapping energy for the small hole polaron (the energy difference between the configuration with the localized hole and the atomic configuration with a delocalized hole) is 0.12 eV.

We find electrons in the conduction band of V_2O_3 can also localize to form small electron polarons. The localized electron polarons are more stable than the delocalized electron by 0.065 eV. We find the electron localizes on two nearest-neighbor V atoms that are ferromagnetically aligned, as illustrated in Fig. 6(b). This polaron configuration, where the extra electron resides on V dimers that are ferromagnetically coupled instead of a single V atom, is often referred to as a Zener polaron.[36] In this configuration the ferromagnetically coupled V-dimers on which the electron polaron resides have a bond length that is 3.4% shorter than the equilibrium V-V bond length within the $a-c$ plane. We also considered the possibility of stabilizing a Zener polaron where the two V atoms are aligned antiferromagnetically. We find this configuration of the self-trapped electron polaron to be 0.016 eV per V atom higher in energy.

Since U, a calculation parameter whose value is only known empirically, can affect the energy of the polaron, it is pertinent to question if the self-trapped polaron is indeed the ground state configuration in the case of electron and hole doped V_2O_3. To verify that this is indeed the case we evaluated the self-trapping energy of small electron and hole polarons in V_2O_3 as a function of the on-site potential U starting from the lowest value of U=1.3 eV which leads to a gap in the V_2O_3 monoclinic structure. For values of U from 1.3 eV to 5 eV, we indeed do find small electron and hole polarons to be more sta-

ble compared to the delocalized state. In the case of the electron polaron we find a transition from the electron being localized on a V dimer to being localized on a single V atom. This is accompanied by an increase in the V-V nearest-neighbor bond length. This is consistent with the competition between intersite hopping between the ferromagnetically aligned V dimers and Hund's exchange[37] and is an effect that has been predicted to occur in other transition metal oxides.

Since we find self-trapped small polarons to be more stable than delocalized electrons or holes, carrier transport measurements in the insulating state of V_2O_3 would lead to hopping-like transport of the polarons between neighboring V sites.[38] This hopping transport of small polarons will have a characteristic activation energy that can be extracted from the temperature-dependent measurements of the conductivity. First-principles calculations of polaron migration barriers yield an upper limit to the activation energy for transport by small polarons.[39] To understand how electron polarons move through the V_2O_3 lattice, we identify two adjacent pairs of V sites where an electron polaron is stable and is localized on a V dimer. We then use a linear interpolation of the two structures and calculate the total energy of each intermediate structure. We find the migration barrier for electron polarons to be 0.09 eV. We apply a similar approach to determine the migration barrier for hole polarons and find it to be 0.11 eV. Hence, we suggest temperature-dependent measurements of carrier transport in the insulating phase of V_2O_3 would observe evidence of hopping transport with an activation energy of $\sim$0.1 eV that can attributed to the presence of small polarons in the material.

IV. SUMMARY AND CONCLUSIONS

In conclusion, we examined the role of Frenkel defects and their influence on the MIT in the vanadates, in particular, focusing on the observation by Ramirez *et al.*[9] that the MIT collapses in V_2O_3 while it remains robust in VO_2.

From our calculations, the following scenario emerges: The recently discovered[22] unique property of the MIT in V_2O_3 is that the transition occurs between a highly frustrated paramagnetic phase with a very low intrinsic Néel temperature, and a strongly antiferromagnetic phase with a very high intrinsic Néel temperature, and is therefore strongly first order. As a result, the transition temperature and its very existence are highly sensitive to the magnetic ordering energy in the low-temperature phase. We have shown that the structural disruptions introduced by defects in the form of Frenkel pairs strongly reduce this energy and thus shift the energy balance toward the HT metallic phase. Vanadium and oxygen Frenkel defects in V_2O_3 decrease the spin-flip energy by up to a factor of 3 compared to pristine V_2O_3. We find the V Frenkel defects to have a lower formation energy than the O Frenkel defects where the vanadium self interstitial in the V Frenkel leads to a ferromagnetically aligned pentamer. We suggest V Frenkel defects are more likely to form in irradiated V_2O_3.

The physics of VO_2 is very different. We have shown that the vacancy and interstitial formed when displacing vanadium atoms lead to a single undimerized V and a dimer-interstitial trimer, leaving the dimers away from either defect intact. The unpaired electrons that are part of V Frenkel defect are localized, and lead to a small gap when subject to Hubbard correlations. We suggest the presence of V Frenkel defects in the insulating phase of VO_2 would lead to a reduction in the resistivity compared to pristine VO_2. Oxygen Frenkel defects due to O displacement leads to the unpaired oxygen interstial forming a bond with a single vanadium atom. This is the lowest energy configuration of the O Frenkel defect. We find all configurations of the O Frenkel defects that we investigated to close the VO_2 band gap. However, we find oxygen Frenkel pairs to have a higher formation energy, at least for the concentrations we considered. We speculate that O defects form in a smaller amount (due to a higher formation energy) and also heal faster, so their concentration is much smaller than the 0.9%, as considered in our calculations. The resulting concentration must be too small to affect macroscopic transport properties of VO_2.

Our second result is that in the insulating phase of V_2O_3 we find small polarons to be stable, either assisted by the presence of defects or as a self-trapped species. Self-trapped small polarons in V_2O_3 can lead to hopping-like conductivity; we find a migration barrier of 0.09 eV for small hole polarons and 0.11 eV for electron polarons. We propose temperature-dependent electrical or optical conductivity measurements in the insulating phase of V_2O_3 would be instrumental in elucidating the presence of small polarons in this material.

ACKNOWLEDGMENTS

D.W acknowledges support from the National Research Council fellowship at the US Naval Research Laboratory. The work of N.B and I.I.M was supported by the Laboratory-University Collaboration Initiative of the DoD Basic Research Office.

[1] T. Rice and D. McWhan, IBM Journal of Research and Development **14**, 251 (1970).

[2] J.-H. Park, L. Tjeng, A. Tanaka, J. Allen, C. Chen, P. Metcalf, J. Honig, F. de Groot, and G. Sawatzky, Phys. Rev.

B **61**, 11506 (2000).
[3] F. Morin, Phys. Rev. Lett. **3**, 34 (1959).
[4] J. Wu, Q. Gu, B. S. Guiton, N. P. de Leon, L. Ouyang, and H. Park, Nano Lett. **6**, 2313 (2006).
[5] D. McWhan, A. Menth, J. Remeika, W. Brinkman, and T. Rice, Phys. Rev. B **7**, 1920 (1973).
[6] D. McWhan, J. Remeika, T. Rice, W. Brinkman, J. Maita, and A. Menth, Phys. Rev. Lett. **27**, 941 (1971).
[7] D. McWhan, T. Rice, and J. Remeika, Phys. Rev. Lett. **23**, 1384 (1969).
[8] K. Appavoo, D. Y. Lei, Y. Sonnefraud, B. Wang, S. T. Pantelides, S. A. Maier, and R. F. Haglund Jr, Nano Lett. **12**, 780 (2012).
[9] J. G. Ramirez, T. Saerbeck, S. Wang, J. Trastoy, M. Malnou, J. Lesueur, J.-P. Crocombette, J. E. Villegas, and I. K. Schuller, Phys. Rev. B **91** (2015), 10.1103/physrevb.91.205123.
[10] V. Eyert, Annalen der Physik **11**, 650 (2002).
[11] J. M. Longo and K. P, Acta Chemica Scandinavica **24**, 420 (1970).
[12] S. Biermann, A. Poteryaev, A. Lichtenstein, and A. Georges, Phys. Rev. Lett. **94**, 026404 (2005).
[13] J. B. Goodenough, Phys. Rev. **117**, 1442 (1960).
[14] J. P. Perdew and M. Levy, Phys. Rev. Lett **51**, 1884 (1983).
[15] L. Sham and M. Schlüter, Phys. Rev. Lett **51**, 1888 (1983).
[16] I. Kylänpää, J. Balachandran, P. Ganesh, O. Heinonen, P. R. Kent, and J. T. Krogel, Phys. Rev. Mat. **1**, 065408 (2017).
[17] Z. Zhu and U. Schwingenschlögl, Phys. Rev. B **86**, 075149 (2012).
[18] C. Weber, D. D. ORegan, N. D. Hine, M. C. Payne, G. Kotliar, and P. B. Littlewood, Phys. Rev. Lett. **108**, 256402 (2012).
[19] C. Chang, T. Koethe, Z. Hu, J. Weinen, S. Agrestini, L. Zhao, J. Gegner, H. Ott, G. Panaccione, H. Wu, *et al.*, Phys. Rev. X **8**, 021004 (2018).
[20] F. Rodolakis, P. Hansmann, J.-P. Rueff, A. Toschi, M. Haverkort, G. Sangiovanni, A. Tanaka, T. Saha-Dasgupta, O. Andersen, K. Held, *et al.*, Phys. Rev. Lett. **104**, 047401 (2010).
[21] L. Paolasini, C. Vettier, F. De Bergevin, F. Yakhou, D. Mannix, A. Stunault, W. Neubeck, M. Altarelli, M. Fabrizio, P. Metcalf, *et al.*, Phys. Rev. Lett. **82**, 4719 (1999).
[22] J. Leiner, H. O. Jeschke, R. Valentí, S. Zhang, A. Savici, J. Lin, M. Stone, M. Lumsden, J. Hong, O. Delaire, *et al.*, Phys. Rev. X **9**, 011035 (2019).
[23] Q. Han and A. Millis, Phys. Rev. Lett. **121**, 067601 (2018).
[24] B. Kim, P. Liu, and C. Franchini, Phys. Rev. B **95**, 024406 (2017).
[25] F. Lechermann, N. Bernstein, I. I. Mazin, and R. Valentí, Phys. Rev. Lett. **121**, 106401 (2018).
[26] P. E. Blöchl, Phys. Rev. B **50**, 17953 (1994).
[27] G. Kresse and J. Hafner, Phys. Rev. B **47**, 558 (1993).
[28] G. Kresse and J. Furthmüller, Phys. Rev. B **54**, 11169 (1996).
[29] J. P. Perdew, K. Burke, and M. Ernzerhof, Phys. Rev. Lett. **77**, 3865 (1996).
[30] V. I. Anisimov, I. Solovyev, M. Korotin, M. Czyżyk, and G. Sawatzky, Phys. Rev. B **48**, 16929 (1993).
[31] M. M. Qazilbash, A. Schafgans, K. Burch, S. Yun, B. Chae, B. Kim, H.-T. Kim, and D. Basov, Phys. Rev. B **77**, 115121 (2008).
[32] R. Moon, Phys. Rev. Lett. **25**, 527 (1970).
[33] P. Dernier and M. Marezio, Phys. Rev. B **2**, 3771 (1970).
[34] B. Medasani, M. L. Sushko, K. M. Rosso, D. K. Schreiber, and S. M. Bruemmer, J. Phys. Chem. C **121**, 1817 (2017).
[35] B. K. Medasani, M. L. Sushko, K. M. Rosso, D. K. Schreiber, and S. M. Bruemmer, J. Phys. Chem. C (2018).
[36] J.-S. Zhou and J. Goodenough, Phys. Rev. B **62**, 3834 (2000).
[37] S. V. Streltsov and D. I. Khomskii, Proc Natl Acad Sci **113**, 10491 (2016).
[38] T. Holstein, Annals of physics **8**, 325 (1959).
[39] T. Maxisch, F. Zhou, and G. Ceder, Phys. Rev. B **73**, 104301 (2006).